접착 및 계면 제7권 제3호, 2006년
〈연구논문(Original Articles)〉

Journal of Adhesion and Interface
Vol.7, No.3, 2006

Synthesis and Characterization of Cu^{2+}-Perfluorophthalocyanine Incorporated SBA15

Mi-Ok Oh, Sung Soo Park, and Chang-Sik Ha†

Department of Polymer Science and Engineering, Pusan National University, Busan 609-735, Korea
(Received June 27, 2006; Accepted July 31, 2006)

Abstract: After anchoring 3-(2-aminoethylamino)propyltriethoxysilane (APTES) onto the surfaces of the channels within ordered mesoporous silica, SBA-15, we dispersed Cu^{2+}-perfluorophthalocyanine into the modified SBA-15 channels. From small-angle X-ray scattering (SAXS) patterns and transmission electron microscopy (TEM) images, we confirmed that both the calcined and Cu^{2+}-perfluorophthalocyanine-incorporated SBA-15 samples possessed ordered periodic structures and hexagonal symmetry lattices (*p6mm*). The value of the d_{100} spacing was decreased after the incorporation of Cu^{2+}-perfluorophthalocyanine into the modified SBA-15 channels. We used FTIR and UV-Vis spectroscopy and thermogravimetric analysis (TGA) to characterize both the modified SBA-15 and the Cu^{2+}-perfluorophthalocyanine-incorporated SBA-15 samples. From scanning electron microscopy (SEM) images and N_2 sorption measurements, we found that the Cu^{2+}-perfluorophthalocyanine units were incorporated within the modified SBA-15 channels, rather than on the external surfaces of the modified SBA-15 channels.

Keywords: The modified SBA-15 channels, Cu^{2+}-perfluorophthalocyanine, post-synthesis, large pores, template-free

1. Introduction

Mesoporous silica, named "M41S" and "SBA series", was synthesized using a surfactant and a triblock copolymer as a template to organize the structure of a polymerizing silica precursor[1]. SBA-15 has larger pores (45～300 Å), thicker walls (30～70 Å), and higher thermal stability than does MCM-41 [1(b)]. These mesoporous molecular sieve materials have found a new range of applications in the areas of catalysis, inclusion chemistry, adsorption, and separation [2-4]. The structural features of the mesoporous materials–very high surface areas (>1000 m^2g^{-1}), ordered nanopore structures, narrow pore size distributions and hydroxyl-covered surfaces–make them excellent candidates for the development of new functional materials. Modification method of mesopores surface via post-synthesis grafting–the incorporation of guest functional molecules into the pores of mesoporous materials–is used widely to modify materials' surface chemistry and to provide active sites for further reactions[5-8]. Quite recently, mesoporous materials have attracted interest for optical applications[9] because the mesopore size range provides several possible advantages to such systems. For example, the high surface area can play a favorable role to prevent aggregation between dope molecules in mesopores at high concentrations. In addition, the mesoscale size range (20～300 Å) is attractive for producing size-confined structures such as quantum dots and nanowires.

Copper phthalocyanine (CuPc) and its derivatives are materials of particular interest in many fields because of their unique electrical and optical properties and their chemical and thermal stability[10,11]. They are of interest for a number of applications, including their use in photovoltaic and solar cells, electrophotographic materials, optical recording and nonlinear optical materials, and sensors[12-15]. For many practical applications, not only the property of the material itself is important but also the degree of dispersion and ordering. Xiong *et al.* applied CuPc into a silica xerogel matrix to fabricate CuPc-based solid state optical devices[16]. The degree of aggregation of CuPc derivatives can affect their linear absorption spectra and change the yields of their photochemical processes. Armengol and co-workers[17] reported the synthesis and catalytic function (toward the oxidation of cyclohexane) of Cu^{2+}-phthalocyanine within the pores

† Corresponding author: e-mail: csha@pusan.ac.kr

of ion exchanged zeolites and MCM-41 aluminosilicate. Zhu *et al*.[18] and Zhou *et al*.[19] synthesized CuPc-doped and surfactant-containing MCM-41 samples through in situ micelle-assisted incorporation of CuPc during the synthesis of MCM-41. But, surfactant-containing MCM-41 samples in the mesopores have limitations in applications of nano-sized mesoporous channels. Moreover, products prepared by post-synthesis grafting are often structurally better defined and hydrolytically more stable than samples prepared by the direct synthesis method.

In this paper, therefore we report that Cu^{2+}-perfluorophthalocyanine ($CuPcF_{16}$) can be dispersed well within modified SBA-15 channels that have larger pores and are free of template by post-synthesis grafting method. Such $CuPcF_{16}$-incoporated mesoporous channels result in photosensitive functional materials that may have potential application in the fields of optics and photonics.

2. Experimental

2.1. Materials

Tetraethoxyorthosilicate (TEOS), poly(ethylene oxide)-*block*-poly(propylene oxide)-*block*-poly(ethylene oxide) ($EO_{20}PO_{70}EO_{20}$, P123), sodium chloride (NaCl), 3-aminopropyltriethoxysilane [$H_2N(CH_2)_3Si(OC_2H_5)_3$, APTES], copper (II) 1,2,3,4,8,9,10,11,15,16,17,18,22,23,24,25-hexadecafluoro-29*H*,31*H*-phthalocyanine ($CuPcF_{16}$) and chloroform were purchased from Aldrich and used without further purification. Hydrochloric acid was purchased from Junsei and used as received.

2.2. Synthesis of SBA-15[20]

In a typical synthesis, the triblock copolymer P123 (1.2 g) and NaCl (4.0 g) were dissolved in water (5.7 g) and 2.0 M HCl (35.0 g) while stirring at 40°C. TEOS (2.0 g) was added to this homogeneous solution and then the mixture was stirred for 24 h at the same temperature. The resulting mixture was transferred into a Teflon-lined autoclave and heated at 80°C for an additional 24 h. The solid products were collected by filtration, washed with distilled water and air-dried at room temperature. The as-synthesized sample was calcined at 500°C for 3 h in air.

2.3. Modification of Calcined SBA-15 Channels[21]

Calcined SBA-15 (0.1 g) was degassed at 300°C for 12 h in a vacuum (ca. 10^{-3} torr), mixed with a chloroform solution of APTES (10 mL, 0.1 M) and then stirred at room temperature for 16 h. The product was filtered, washed with chloroform and then dried at room temperature. This sample was named "APTES/SBA-15".

2.4. Incorporation of $CuPcF_{16}$ into Modified SBA-15 Channels

The modified SBA-15 (0.1 g) and $CuPcF_{16}$ (2 wt%) were dissolved in chloroform (10 mL). The mixture was stirred continuously for 48 h at room temperature and then filtered and washed with chloroform. The final product was dried at room temperature. This sample was named "$CuPcF_{16}$/APTES/SBA-15".

2.5. Characterization

Small-angle X-ray scattering (SAXS) was performed at the Pohang Accelerator Laboratory (PAL), Korea, using Co Kα (λ=1.608 Å) radiation. Nitrogen adsorption and desorption isotherms were measured at 77 K using a Micromeritics ASAP 2010 equipped with an accelerated surface area and a micropore analysis system. Prior to measurement, the samples were dehydrated at 150°C for 24 h. Samples in KBr pellets were characterized by FTIR spectroscopy under ambient conditions. All spectra were recorded using a JASCO FT/IR-460 Plus FTIR spectrometer. Transmission electron microscopy (TEM) images were obtained using a JEOL JEM-2010 electron microscope operated at 200 kV. The morphologies of the samples were obtained using a Hitachi S-4200 scanning electron microscope (SEM). Prior to imaging, the samples were coated with gold through the use of a Hitachi E-1010 sputter coater. UV-Vis diffuse reflectance spectra (DRUV) were measured using a Kontron Instrument Uvikon 860 spectrophotometer.

3. Results and Discussion

The calcined SBA-15 sample (Figure 1a) exhibits three well-resolved peaks (a prominent peak at q = 0.6 nm^{-1} and two weak peaks at 1.1 and 1.3 nm^{-1}) that can be indexed to the (100), (110), and (200) reflections of a hexagonal symmetry lattice (*p6mm*) possessing d-spacings of 10.0, 5.8 and 5.0 nm, respectively. The corresponding unit cell parameter a_o is 116 Å [$a_o = 2d_{100}/\sqrt{3}$]. Figure 1b indicates that the modified SBA-15 sample (APTES/SBA-15) also possesses a well-ordered hexagonal mesoporous structure that exhibits similar peaks to that of the

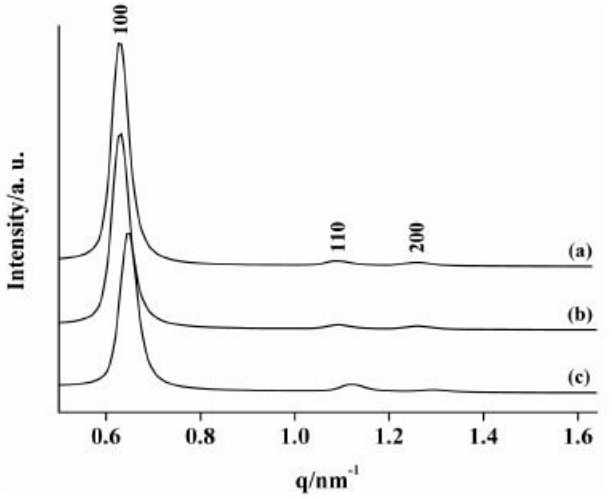

Figure 1. Small-angle X-ray scattering (SAXS) patterns of (a) calcined SBA-15, (b) APTES/SBA-15 and (c) $CuPcF_{16}$/APTES/SBA-15.

calcined SBA-15; the intensities of the peaks, however, decreased after modification. Furthermore, as demonstrated in Figure 1c, the (100) peak shifted to a higher angle after the incorporation of $CuPcF_{16}$. The d_{100} spacing of this sample was 9.7 nm and the unit cell parameter was 112 Å. The decreases in the peak intensities and their shifts to higher angles are due to filling of the pores of SBA-15 during the incorporating process because such pore filling reduces the scattering contrast between the pores and the walls of mesoporous material. We note that even after incorporating $CuPcF_{16}$ into the modified SBA-15 channels (i.e., for $CuPcF_{16}$/ APTES/ SBA-15), the well-ordered hexagonal mesostructure was retained: the three well-resolved peaks still can be indexed to the (100), (110), and (200) reflections.

Figure 2 displays the nitrogen adsorption/desorption isotherms of the (a) calcined SBA-15 and (b) $CuPcF_{16}$/ APTES/SBA-15 samples. After incorporation of $CuPcF_{16}$ into the modified SBA-15 channel (i.e., for $CuPcF_{16}$/ APTES/SBA-15), we observed a decrease in the amount of nitrogen adsorbed and a shift in the inflection point of the step to a smaller relative pressure (Figure 2b). We attributed the reduced nitrogen adsorption to the smaller specific surface area and the lower relative pressure to the decreased pore size[22]. After incorporation of $CuPcF_{16}$ within the mesoporous channels, the pore diameter decreased from 6.4 to 5.8 nm (Figure 3). These observations indicate that $CuPcF_{16}$ was incorporated successfully into the modified SBA-15 channels.

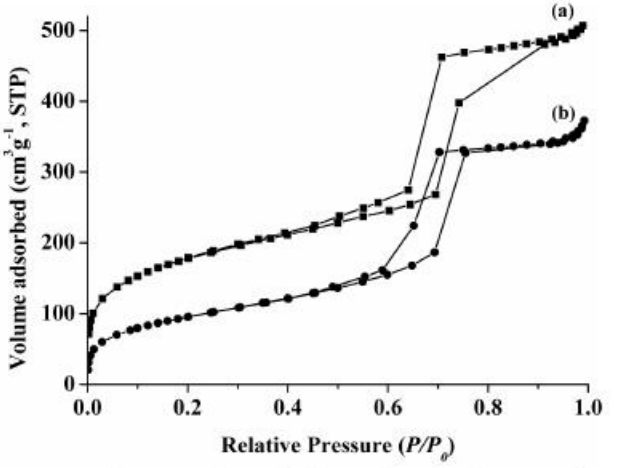

Figure 2. Nitrogen adsorption/desorption isotherms of (a) calcined SBA-15 and (b) $CuPcF_{16}$/APTES/SBA-15.

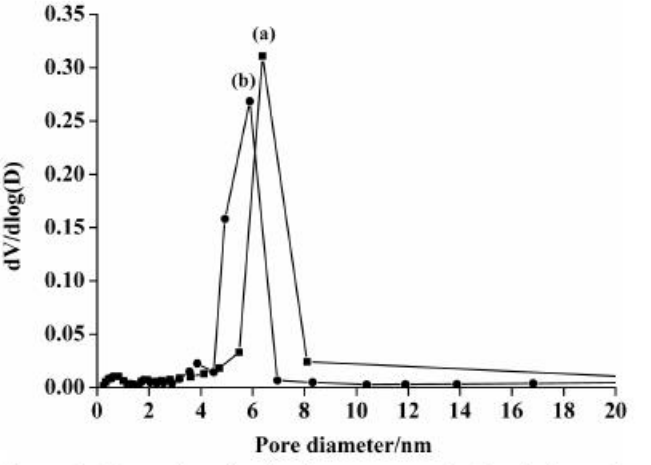

Figure 3. Pore size distribution curves calculated from the nitrogen desorption branch of the isotherms of (a) calcined SBA-15 and (b) $CuPcF_{16}$/APTES/SBA-15.

Figure 4 displays the FTIR spectra of (a) calcined SBA-15, (b) APTES/SBA-15, (c) $CuPcF_{16}$/APTES/SBA-15 and (d) pure $CuPcF_{16}$. For all of these samples, bands are clearly visible at 1085 and 803 cm^{-1}, and 460 cm^{-1} for the Si-O-Si framework. The pronounced absorption at 970 cm^{-1} indicates Si-OH stretching. Figure 4b indicates that the IR spectrum of the modified SBA-15 (i.e., that of APTES/SBA-15) exhibits additional peaks for CH_2 stretching (2943 cm^{-1}), CH_2 bending (1473 cm^{-1}) and N-H bending (1530 cm^{-1}) relative to that of the calcined SBA-15 (Figure 4a). Pure CuPcF16 exhibits C=N absorptions at 1741 and 1706 cm^{-1}, aromatic C=C stretching absorptions at 1524 and 1488 cm^{-1} and a C-F absorption at 1151 cm^{-1} (Figure 4d). $CuPcF_{16}$/APTES/

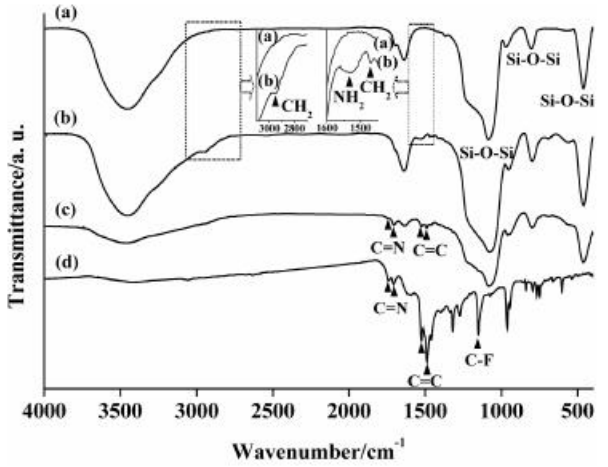

Figure 4. FTIR spectra of (a) calcined SBA-15, (b) APTES/SBA-15, (c) $CuPcF_{16}$/APTES/SBA-15 and (d) pure $CuPcF_{16}$.

SBA-15 exhibits similar absorption bands to those of pure $CuPcF_{16}$, including, for example, peaks for C=N (1740～1500 cm^{-1}) and aromatic C=C bond (1520～1490 cm^{-1}) vibrations (Figure 4c). For the $CuPcF_{16}$/APTES/SBA-15 sample, however, the C-F absorption at 1151 cm^{-1} overlapped with the strong peak for the Si-O-Si vibrations.

Figure 5 displays TEM images of the (a) calcined SBA-15 and (b) $CuPcF_{16}$/APTES/SBA-15 samples. The calcined SBA-15 (Figure 5a) appears to have a well-ordered hexagonal mesostructure (p6*mm*). The TEM image of $CuPcF_{16}$/APTES/SBA-15 (Figure 5b) indicates that this mesostructure retained its well-ordered hexagonal array during the incorporation of $CuPcF_{16}$ into the mesoporous channels; this result is consistent with the SAXS pattern presented in Figure 1c. The particles of the calcined SBA-15 exhibit rod-like shapes and have diameters of ca. 6 μm (Figure 6a). After incorporation of $CuPcF_{16}$ into the modified SBA-15 channels (i.e., after formation of $CuPcF_{16}$/APTES/SBA-15), the rods are thicker than those of the calcined SBA-15, but we do not observe any noticeable particles of $CuPcF_{16}$. The result hints that the $CuPcF_{16}$ moieties are dispersed within the mesopores without agglomeration on the external surfaces of the mesopores (see also Figure 5b), if we consider that the average diameter of pure $CuPcF_{16}$ particles is ca. 8 μm due to the agglomeration in the absence of SBA-15 (see Figure 6d). Figure 6e displays an SEM image of the calcined SBA-15 and $CuPcF_{16}$ after their physical mixing; this image exhibits simply a mixture of the agglomerated particles of $CuPcF_{16}$ (marked with arrows)

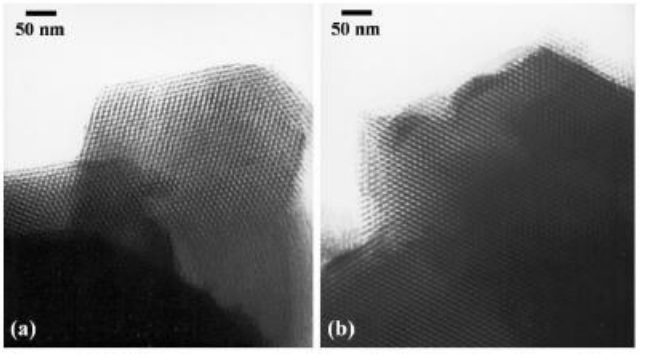

Figure 5. TEM images of (a) calcined SBA-15 and (b) $CuPcF_{16}$/APTES/SBA-15.

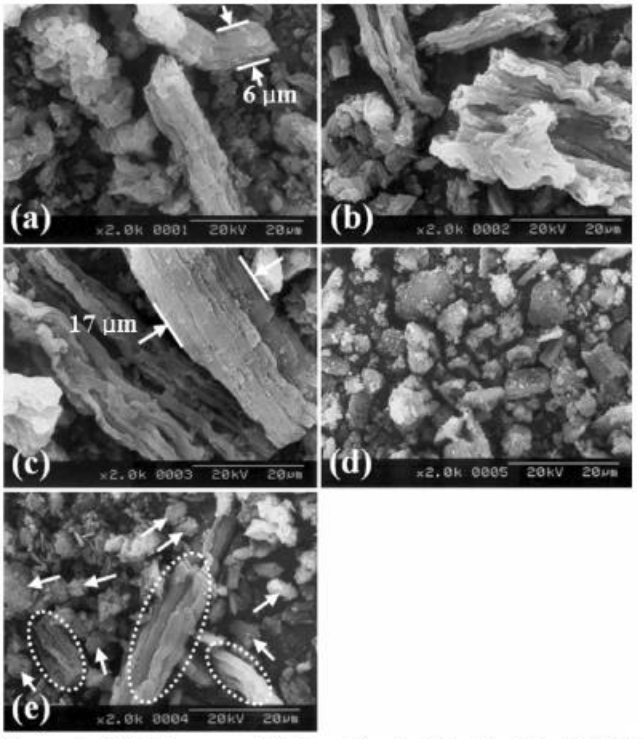

Figure 6. SEM images of (a) calcined SBA-15, (b) APTES/SBA-15, (c) $CuPcF_{16}$/APTES/SBA-15, (d) pure $CuPcF_{16}$ and (e) a physical mixture of calcined SBA-15 and $CuPcF_{16}$.

and the rod-like SBA-15 (marked with dotted circles) units. Accordingly, we conclude that the $CuPcF_{16}$ units were dispersed well within the modified channels of $CuPcF_{16}$/APTES/SBA-15.

We used thermogravimetric analysis (TGA) to investigate the thermal stability of the samples. Figure 7 displays the weight losses of the samples (in percentages) as a function of the temperature. We attribute the weight loss of calcined SBA-15 (Figure 7a) below 100°C to the desorption of physisorbed water (ca. 1.2%), and its weight

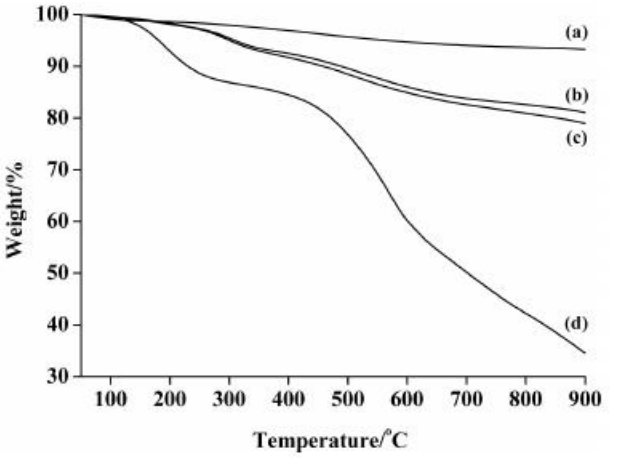

Figure 7. TGA curves of (a) calcined SBA-15, (b) APTES/SBA-15, (c) $CuPcF_{16}$/APTES/SBA-15 and (d) pure $CuPcF_{16}$.

loss upon increasing the temperature up to 900°C to the release of water formed from the condensation of silanol units within the framework[23]; the total weight loss of the sample was 7.8%. The weight losses of the APTES/SBA-15 and $CuPcF_{16}$/APTES/SBA-15 samples below 100 °C were lower because of the number of OH groups that had been modified with the organic moieties[24]. In Figure 7b and 7c, we observe that the noticeable weight losses for APTES/SBA-15 and $CuPcF_{16}$/APTES/ SBA-15 occurred at ca. 300～500°C, which we attribute, in part, to the modification and incorporation of $CuPcF_{16}$ within the channels of SBA-15. The total weight losses of APTES/SBA-15 and $CuPcF_{16}$/APTES/SBA-15 at 900°C were ca. 18.8 and 20.9%, respectively.

Figure 8 displays the UV-Vis absorption spectra of (a) calcined SBA-15, (b) $CuPcF_{16}$/APTES/SBA-15 and (c) pure $CuPcF_{16}$. Our sample of calcined SBA-15 did not exhibit any UV-Vis absorptions (Figure 8a), as expected from the literature[25]. Pure $CuPcF_{16}$ exhibits (Figure 8c) electronic transitions in the visible and near infrared regions (Q-bands at 587, 654, 700 and 797 nm) and in the near ultraviolet region (B-band at 361 nm);[10,11] in addition, we observed a weak satellite band near 600 nm, which we attribute to the higher vibrational levels of the relevant electronic state. The UV-Vis absorption spectrum of $CuPcF_{16}$/APTES/SBA-15 dispersed in ethanol displays (Figure 8b) weak peaks, similar to those in the spectrum of pure $CuPcF_{16}$, at 363, 585, 662, 704 and 797 nm. The absorption peaks of $CuPcF_{16}$/APTES/SBA-15 are not narrow, possibly because of the broad size distribution of the incorporated $CuPcF_{16}$ moieties.

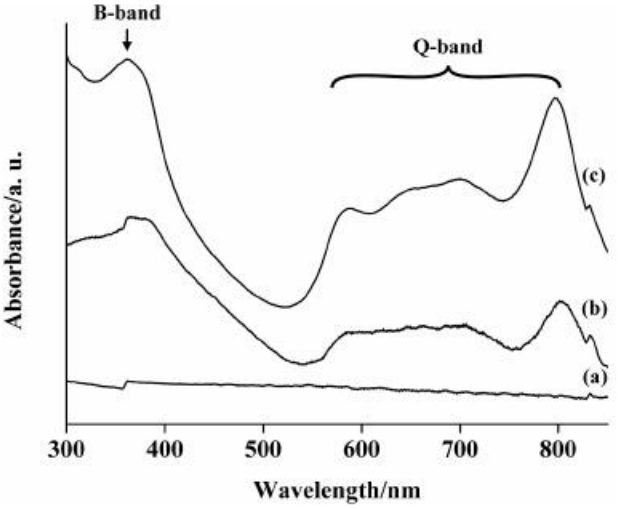

Figure 8. UV-Vis absorption spectra of (a) calcined SBA-15, (b) $CuPcF_{16}$/APTES/SBA-15 and (c) pure $CuPcF_{16}$.

4. Conclusions

We used a post-synthesis method to disperse Cu^{2+}-perfluorophthalocyanine ($CuPcF_{16}$) efficiently into the modified, wide channels of SBA-15. The ordered mesoporous channels provided a microenvironment that prevented aggregation of $CuPcF_{16}$ units. $CuPcF_{16}$-incorporated SBA-15 within large pores may have potential application in the fields of optics and photonics.

Acknowledgements

This study was supported by the National Research Laboratory Program and the SRC/ERC program of MOST/KOSEF; R11-2000-070-080020).

References

1. (a) C. T. Kresge, M. E. Leonowicz, W. J. Roth, J. C. Vartuli, and J. S. Beck, *Nature*, **359**, 710 (1992). (b) D. Zhao, J. Feng, Q. Huo, N. Melosh, G. H. Fredrickson, B. F. Chmelka, and G. D. Stucky, *Science*, **279**, 548 (1998).
2. A. Sayari, Chem. *Mater*., **8**, 1840 (1996).
3. M. Raimondo, G. Perez, M. Sinibaldi, A. de Stefanis, and A. A. G. Tomlinson, *Chem. Commun*., 1343 (1997).
4. M. Grun, A. A. Kruganoz, S. Schacht, F. Schuth, and K. K. Unger, *J. Chromatogr. A*, **740**, 1 (1996).
5. S. Xiang, Y. Zhang, Q. Xin, and C. Li, *Angew*.

Chem. Int. Ed., **41**, 821 (2002).
6. M. J. MacLachlan, P. Aroca, N. Coombs, I. Manners, and G. A. Ozin, *Adv. Mater.*, **10**, 144 (1998).
7. J. Liu, X. D. Feng, G. E. Fryxell, L. Q. Wang, A. Y. Kim, and M. L. Gong, *Adv. Mater.*, **10**, 161 (1998).
8. G. J. Kim, H. S. Kim, Y. S. Ko, and Y. K. Kwon, *Macromol. Res.*, **13**(6), 499 (2005).
9. B. J. Scott, G. Wirnsberger, and G. D. Stucky, *Chem. Mater.*, **13**, 3140 (2001).
10. A. Stein, B. J. Melde, and R. C. Schroden, *Adv. Mater.*, **12**, 1403 (2000).
11. G. Guillaud, J. Simon, and J. P. Germain, *Coord. Chem. Rev.*, **178**, 1433 (1998).
12. P. Peumans, A. Yakimov, and S. R. Forrest, *J. Appl. Phys.*, **93**, 3693 (2003).
13. A. Yakimov and S. R. Forrest, *Appl. Phys. Lett.*, **80**, 1667 (2002).
14. V. P. Singh, B. Parsarathy, R. S. Singh, A. Aguilera, J. Anthony, and M. Payne, *Sol. Energy Mater. Sol. Cells*, **90**, 798 (2006).
15. Q. Chen, D. Gu, J. Shu, X. Tang, and F. Gan, Mater. *Sci. Eng. B*, **25**, 171 (1994).
16. G. Xiong, Z. Wang, G. Qian, X. Fan, and M. Wang, *J. Sol-Gel Sci. Technol.*, **18**, 21 (2000).
17. E. Armengol, A. Corma, V. Fornés, and H. Garcia, J. Primo, *Appl. Catal. A*, **181**, 305 (1999).
18. Y. Zhu, S. Ding, Y. Dong, and Y. Hu, *Colloids Surf. A*, **220**, 131 (2003).
19. H. S. Zhou, H. Sasabe, and I. Honma, *J. Mater. Chem.*, **8**, 515 (1998).
20. W. Guo, J. Y. Park, M. O. Oh, H. W. Jeong, W. J. Cho, I. Kim, and C.-S. Ha, *Chem. Mater.*, **15**, 2295 (2003).
21. D. H. Park, S. S. Park, and S. J. Choe, *Bull. Korean Chem. Soc.*, **20**, 291 (1999).
22. C. P. Jaroniec, M. Kruk, M. Jaroniec, and A. Sayari, *J. Phys. Chem. B*, **102**, 5503 (1998).
23. A. S. Maria Chong and X. S. Zhao, *J. Phys. Chem. B*, **107**, 12650 (2003).
24. D. Zhao, Q. Huo, J. Feng, B. F. Chmelka, and G. D. Stucky, *J. Am. Chem. Soc.*, **120**, 6024 (1998).
25. Q. Xu, L. Li, B. Li, J. Yu, and R. Xu, *Micropor. Mesopor. Mater.*, **38**, 351 (2000).